Phage Steering in the Presence of a Competing Bacterial Pathogen

Authors: Sean M. Czerwinski [1], James Gurney [1 *]
Affiliation: [1] School of Biology, Georgia State University, Atlanta, Georgia USA.
* Corresponding author jgurney2@gsu.edu

Abstract

The rise of antibiotic-resistant bacteria has necessitated the development of alternative therapeutic strategies such as bacteriophage therapy, where viruses specifically infect bacteria. However, rapid bacterial resistance to phage treatment remains a critical challenge, often leading to failure. Phage steering, which leverages the co-evolutionary dynamics between phage and bacteria, offers a novel solution by driving bacteria to evolve away from virulence factors or resistance mechanisms. In this study, we examined whether phage steering using bacteriophage Luz19 could function in the presence of a competing pathogen, *Staphylococcus aureus* (USA300), while targeting *Pseudomonas aeruginosa* (PAO1). Through *in vitro* co-evolution experiments with and without the competitor, we observed that Luz19 consistently steered *P. aeruginosa* away from the Type IV Pilus (T4P), a key virulence factor, without interference from *S. aureus*. Genomic analyses revealed mutations in T4P-associated genes, including *pilR* and *pilZ*, which conferred phage resistance. Our findings suggest that Phage Steering remains effective even in polymicrobial environments, providing a promising avenue for enhancing bacteriophage therapy efficacy in complex infections.

Introduction

The increasing prevalence of antibiotic-resistant bacteria necessitates the exploration of alternative therapeutic approaches. Bacterio(phage) therapy, which utilizes viruses that infect and kill bacteria to combat drug-resistant infections, offers a promising avenue. However, the rapid emergence of phage-resistance *in vitro* raises alarms over its long-term efficacy [1, 2]. The antagonistic co-evolutionary dynamics of bacteria-phage interactions generates diversity in both the bacterial and phage populations, with reciprocal evolution of defense vs attack alleles occurring in an almost turn-based competition known as Arms Race Dynamics (ARD) [3-5] wherein bacterial resistance to phage emerges, followed by the evolution of phage infectivity [6-11]. Ultimately, in the lab, ARD culminates in the emergence of a resistant genotype that the phages cannot overcome [8], in most cases coming in the form of *de novo* mutations resulting in the loss or structural and functional attenuation of the specific surface receptors in which the bacteriophage binds [8]. The shortcoming of bacteriophages as a miracle treatment is to be expected, as Lenski and Levin proposed, there is an asymmetry in the evolutionary potential between the bacterium and its phage [8, 9]. This asymmetry is due, in part, to a single spontaneous *de novo* mutation resulting in significant receptor structure alteration and therefore acquisition of resistance for the bacterium, whereas the bacteriophage would need multiple successive *de novo* mutations in order to overcome resistance [12, 13]. Phage Steering seeks to exploit the directional selection of parasite-host coevolution. In the event that resistance evolves against the phage, the *de novo* mutations that result from ARD, should lead to the loss or functional attenuation of the binding receptor [9, 14, 15]. Phage steering utilizes bacteriophages with known receptors, or factors, that are implicated in antimicrobial resistance or in virulence [14].

The intricate dynamics of bacteria-phage interactions, particularly the rapid emergence of phage resistance, pose significant challenges to the long-term efficacy of bacteriophage therapy. This is especially critical when considering pathogens like *Pseudomonas aeruginosa* (*PA*), a notorious

Gram-negative bacterium known for its intrinsic multi-drug resistance and its role in chronic, often life-threatening infections. Furthermore, *PA* infections often occur in a poly-microbial context, most notably alongside *Staphylococcus aureus* (*SA*), significantly complicating treatment strategies. These two pathogens are the most prevalent in cystic fibrosis infections, with studies indicating enhanced virulence when they coexist [16, 17]. The dynamic and often synergistic interactions between *PA* and *SA* in co-infection models [16, 18-21], emphasize the complexity of *PA*-associated polymicrobial infections. The community interactions found within a polymicrobial infection has the potential to greatly impact phage therapies and steering. As previously mentioned, *PA* is an opportunistic pathogen, and did not evolve its vast armament of virulence factors and antimicrobial resistance mechanisms in order to colonize a human host, but rather to outcompete other micro-organisms in the environment. Thus, the question remains whether or not phage steering will prove efficacious in the presence of competing co-infecting organisms that exert their own selective pressure via competition or otherwise interaction.

In this study, we focus on the interplay between *Pseudomonas aeruginosa* - *PA*O1 (*PA)* and *Staphylococcus aureus* - USA300 (*SA*) and the phage Luz19. We employ the phage Luz19 to steer *PA*O1 away from the expression or function of its receptor, the Type IV pilus (T4P) (**Fig. 1**) [22, 23]. By a series of co-evolution lines with and without the phage and *SA* present we determined if Luz19 is able to perform Phage Steering on *PA* during bacterial competition. Our phenotypic assays of T4P activity and whole genome sequencing of evolved lines show that Phage Steering still works under competition with *SA* in LB, it remains to be seen if in media that replicate infection conditions or *in vivo* allow for the action of Phage Steering.

Materials and Methods

Bacterial culture and phage preparation.

Pseudomonas aeruginosa (Nottingham *PA*O1) was grown at 37°C with agitation (shaking at 200 rpm) in Lysogeny Broth (LB) media. For phage stock quantification, Luz19 phage was diluted in 1X Phosphate Buffer Saline (PBS) and spot plated onto *PA*O1 soft lawns on Lysogeny Broth Agar (LBA) and incubated at 37°C overnight. Plaque Forming Units (PFUs) were counted, and PFU/mL was calculated. Phage stock was diluted in 1X PBS. The final concentration of phage stock prior to initial inoculation was approximately 3.0e9 PFU/mL. Phage inoculation dosage was calculated for a multiplicity of infection (MOI) of 3, from estimated Colony Forming Unit (CFU) per mL by multiplying the Optical Density at a wavelength of 600 nm OD_{600} by 8.0e8 (Supplemental data).

In vitro evolution experiment.

We investigated bacterial evolutionary response to an anti-virulence bacteriophage, Luz19, over the course of 10 serial transfers (10 days) in the context of presence or absence of a common competitor, *Staphylococcus aureus* (*SA*). A total of three co-evolution conditions were used, *PA* with *SA*, *PA* with Luz19 phage, and *PA* with both phage and *SA*. A control for serial transfer culturing was included with only *PA* serially transferred for the total 10 transfers. All co-evolution cultures were conducted in 1 ml LB in 24 well plates (Corning)®) and incubated at 37°C, shaking, for 24 hours. Bacteria colony forming unit (CFU) estimates for initial and subsequent (for *SA*) inoculations were made using OD_{600} measurements. For accurate CFU estimation from OD_{600}, *PA*O1 and USA300 suspended cultures were spectrophotometrically measured and then serially diluted and CFU plate counted. An OD_{600}=1.0 was found to contain approximately 8e^8 and 1e8 CFU/mL for *PA*O1 and USA300 respectively. 50 µL of *PA*O1 (1.64e7 CFU) was inoculated into wells containing 900 µL of LB media. In conditions with phage, bacteria were exposed to the 16 µL of the initial ancestral Luz19 phage at an MOI of 3:1

102 (4.91e7 PFU); from Luz19 stock at 3.0e^9 PFU/mL at time point 0 (T0). Stock phage
103 concentrations were previously determined via PFU.
104
105 In conditions with competing *SA,* 50 µL of USA300 *(2.04 e*6 CFU) was inoculated
106 into the wells containing 900uL of LB media and 50 µL of newly inoculated *PA*O1. In +*SA*
107 conditions, 50 µL of *SA*, 5.0e^6 CFUs, was re-introduced at each transfer to maintain the
108 selective pressure generated by consistent competition.
109
110 In pilot experiments, we found that *SA* went extinct after no more than 3 transfers when co-
111 cultured with *PA*O1 at comparable relative concentrations (data not shown). After 24 hours, 100
112 µL was transferred into 900 µL of LB media. 300 µL was stored in 25% final concentration
113 glycerol at – 80˚C.
114
115 In the case that a replicate culture needed to be restarted, the frozen stock was used to resume
116 the replicate from the most recently stored time point. 1 µl of Frozen culture was inoculated into
117 1 mL of LB and incubated with shaking for 4 hours. 100µL was then transferred into 900 µL of
118 LB and normal culturing conditions resumed. Upon culmination of co-evolution culturing, all
119 Transfer 10 replicates were frozen in glycerol (25% final) and stored at -80˚C.
120
121 **Preparation for Twitching Motility and Growth Rate Assays.**
122 Frozen replicates were cultured in LB at 37°C shaking overnight. The overnight culture was then
123 transferred into a 1.5 mL microfuge tube, vortexed to break up aggregates, and then centrifuged
124 at 17,000 RCF for 2 minutes to pellet the cells then washed 2 times in 1X PBS and re-pelleted.
125 Cells were resuspended in 1 mL of LB and further diluted in LB to an OD_{600} of 0.05. In the case
126 of USA300-positive co-cultures, cultures were streaked onto Pseudomonas Isolation Agar (PIA)
127 and incubated at 37°C overnight to remove *SA*. Single colonies of isolated *PA* were incubated
128 overnight at 37°C in LB.
129
130 **qPCR of Phages.**
131 qPCR of phage stock was performed using the QuantStudio 3 rt PCR system and analyzed with
132 the ThermoFisher applied biosystems app. See SI for list of primers used.
133
134 **Twitching Motility Assays.**
135 We performed a twitching motility assay adapted from Alm & Mattick's 1996 protocol, with the
136 following modifications [24]. A p20 pipette tip was introduced to the cultures then pushed
137 through a LB agar plate until the pipette tip contacted plastic at the base of the plate and then
138 promptly removed. Plates were incubated at 37°C for 20 h. Agar was removed to reveal the
139 imprint of *PA* growth. Imprints were stained with Crystal Violet for 15 min. Excess stain was
140 gently washed off using sterile diH_2O. Plates were then air dried. Once dry, the stained imprints
141 were measured across at the widest point. All phenotypic assays were done in triplicate for each
142 co-evolution replicate for a total of 15 assay replicates-per-condition.
143
144 Data transformations (log and Box-Cox using the car package for R 4.2.2 [25]) were attempted,
145 but normality was not achieved across all treatments according to a Shapiro-Wilk test. Due to
146 heteroskedasticity we used the Kruskal-Wallis test. When significant differences were found,
147 post-hoc analyses were performed using the Games-Howell test for Welch's ANOVA.
148
149 **Growth Rate Analysis.**
150 Analysis of growth rate assays was performed using the Growthcurver package for R [26].
151 Growthcurver fits the data points collected for each individual replicates growth curve to a
152 standard form of the logistics equation used in ecology and evolution [26]. Growth rate curves

had the area under the logistic growth curves differentiated for each co-evolution condition subject to four different growth rate treatments, with standard error bars. AUC(l) is calculated as the area under the logistic curve obtained by integrating the logistic equation using the growthcurver package [26].

The growth rates of (*PA*) from different co-evolution conditions under various treatments was assessed via area under the curve AUC(l). Statistical analyses were performed to determine significant differences in growth between conditions and treatments. Data transformations (log and Box-Cox using 'car' and 'MASS' packages for R 4.2.2 respectively[25]) were attempted but did not achieve normality across all treatments. The Kruskal-Wallis test was used when significant differences were found, post-hoc analyses were performed using Games-Howell test for Welch's ANOVA and Dunn's test with Bonferroni correction for Kruskal-Wallis. There was no difference in the control evolution line (**SI Fig. 1**) We also performed the same analysis on growth rate (r) and carrying capacity (k) (**SI Fig. 2 & 3**).

DNA Extraction & Purification.
Single colonies were cultured in LB shaking overnight at 37°C. DNA extraction, isolation, and purification was performed using the Promega Wizard ® Genomic DNA Purification Kit following the manufacturer's instructions.

Sequencing.
Whole genome sequencing of replicates was performed by SeqCoast Genomics (Portsmouth, NH, USA). SeqCoast prepared samples using the Illumina DNA Prep tagmentation kit and unique dual indexes. Sequencing was performed on the Illumina NextSeq2000 platform using a 300-cycle flow cell kit to produce a 2x150bp paired reads. 1-2$ PhiX control was spiked into the run to support optimal base calling. Read demultiplexing, read trimming, and run analytics were performed using DRAGEN v3.10.12, an on-board analysis software on the NextSeq2000.

Genomic Analysis.
Genomic analyses were completed using breseq 0.38.3 [27] computational pipeline to identify mutations relative to the reference *PA*O1 genome Pseudomonas aeruginosa PAO1 [28]. Sequencing of our ancestral n*PA*O1 genome and subsequent breseq analysis was used to identify single nucleotide polymorphisms (SNPs) that are not present in the reference genome [28]. We compared the ancestral nPAO1 to the evolved *PA* to remove SNPs that were a result of adaptation to the media.

Results
Twitching Motility.
Selection by Luz19 phage attenuates twitching motility function in the presence of competing *SA* (**Fig. 2**). Twitching motility was attenuated in phage-positive conditions in the presence and absence of competing *SA* ($p < 0.05$ for both conditions), relative to the ancestral WT. There was not significant difference between the two positive-phage conditions nor between the WT ancestor and the negative/negative culture control. *PA* that was co-cultured with *SA* did not have a significant difference in twitching motility relative to the WT control ($p > 0.05$).

Growth rate assays and area under the curve.
Our statistical analysis asked two questions. First – did strains evolved under phage selection develop resistance. We found no significant difference in the area under the curve of lines evolved with the phage compared when tested with and without the phage present. When compared to the ancestor there was a significant reduction in growth in the ancestor when phages were present (**Fig. 3**). Second, did the evolution in the media or in the presence of *SA*

alter phage resistance. Our analysis revealed significant differences in the area under the growth curve among the co-evolution conditions (χ^2=54.54, *df* = 4, p = 4.06e−11) (**Fig 4**). Subsequent Dunn's post-hoc tests with Bonferroni correction were performed to identify specific condition differences within the assay treatments. When exposed to the ancestral phage, our data shows that only lines evolved in the presence of the phage demonstrated increased resistance, as measured by area under the curve. This increased resistance was observed in both the +Luz19 and +*SA*+Luz19 treatments compared to the ancestral *PA*O1 strain (p = 2.17 e-04 and p = 3.47e-05, respectively). Importantly, the presence of S. aureus during evolution did not significantly alter phage resistance. There was no significant difference between the +Luz19 and +*SA*+Luz19 treatments (p > 0.05), indicating that co-evolution with *S. aureus* did not alter resistance against the phage. Neither *S. aureus* co-culture nor the media alone increased resistance to the phage (p > 0.05). These results consistently demonstrate the enhanced phage resistance in evolved lines, regardless of the presence of *SA* during evolution.

Genomics.

Sequencing revealed a clear signature of evolution in the presence of the phage (**Fig. 5**). Three SNP variations between two genes involved in Type 4 Pilus biogenesis, *pilR* and *pilZ,* were defined in the conditions subject to coevolution with the phage. In the two conditions with phage, 8 out of 10 replicates (5/5 +Phage, 3/5 +Phage/+*SA*) had SNPs in *pilR*, the response regulator element of the PilSR two component system, responsible for activation of *pilA* transcription [29].

Of the remaining two replicates, one (replicate A) had a 197 bp deletion in *pilZ*. The Δ197bp *pilZ* replicate showed significantly attenuated twitching motility (p < 0.05) with no significant motility difference between it and the *pilR* mutants (**Fig. 5**).

Replicate B of the +Phage+*SA* condition lacked detectable SNPs in genes directly related to Type 4 pilus biogenesis, structure, or function. However, it did have a unique SNP in *mvfR*, also known as *pqsR*, which is a global virulence regulator implicated in quorum sensing [30]. It is currently unclear what specific impact the *mvfR* mutation has on T4P expression or function, though the replicate did show roughly the same attenuation of twitching motility (**Fig. 2**) and followed resistant growth curves (**Fig. 5**)

Discussion

Phage Steering is the use of phage to reduce or remove pathogenic behaviors from a bacterial population. Fundamentally, it works by phage making use of a bacterial product, typically an outer membrane expressed structure, in some way to complete a full infection cycle. Bacteria are therefore under a selective pressure to modify the structure – engendering resistance to the phage. This modification also typically leads to a reduction in effectiveness of the structure in its evolved function. Should the structure not provide an actual fitness benefit in the environment in which the phage is applied there is no selective pressure to restore the phenotype. In infections like those seen in the Cystic Fibrosis lung, many virulence factors of *PA* do not provide a fitness benefit when considered in isolation, only contributing to nonadaptive virulence, increasing morbidity of people with CF. This is likely due to *PA* not having evolved in the CF lung, as the CF lung itself is, in evolutionary terms, incredibly young. Before 1930s the majority of people with CF died before lung became chronically infected with *PA* [31]. However, virulence factors such as the Type 4 Pili likely did evolve to help bacteria deal with inter species competition. Therefore, a central requirement of Phage Steering, the lack of fitness consequence during phage application might not hold true if *PA* is competition with other bacteria at the time of phage application.

255 We aimed to test the question of how phage steering works during multispecies competition, we
256 did so in a simple experimental setup, effectively providing Phage Steering with the most
257 favorable conditions to work. A simple co-evolutionary experiment with either the phage, Luz19,
258 or *SA*, or in combination or in the absence of either. The major result of our work is that
259 regardless of the presence of *SA,* the phage still steered *PA* away from the expression of type 4
260 pili, there was also no clear example of mutations outside the those that control type 4 pili in
261 either case when *SA* was present. We measured the phenotypic changes in T4P with twitching
262 motility, we confirmed phage resistance emerged as effectively in both phage treatments,
263 indicating again the presence of *SA* did not alter this outcome. Finally, we genomically
264 characterized individual isolates after the evolution experiment and found the mutations
265 selected by Luz19 were found in pili structural and regulatory genes.
266
267 Examining these specific mutations in more detail, the gene product of *pilA*, is the major
268 subunit, pilin (PilA) that composes the Type 4 pilus shaft [32, 33]. PilS is located within the
269 inner membrane of *PA* and is responsible for the detection of excess pilin/PilA subunits
270 localized to the inner membrane [29]. In the absence of excess PilA, PilS autophosphorylates,
271 and subsequently transfers the phosphate group to the regulator protein, PilR [29]. PilR then
272 binds to a specific sequence proximal to the promoter of *pilA;* and with the assistance of the
273 alternative sigma factor, σ54, *pilA* is transcribed [29] (**Fig. 6**). Two unique SNPs in *pilR* were
274 found in the phage-positive replicates, both point substitutions that result in amino acid
275 changes. Of the eight *pilR* SNPs, seven were C192Y(TGC→TAC) with the sole outlier,
276 P189Q (CCG→CAG). There was no significant difference between the attenuation of twitching
277 motility between the two *pilR* mutation variants. The gene product of *pilZ* is another regulatory
278 element of type 4 pilus biogenesis [34]. PilZ interacts with PilB, an AT*Pa*se localized to the
279 cytoplasmic face of the inner membrane that provides the energy necessary to transfer the pilin
280 subunits from the inner membrane to the base of the growing pilus polymer [34]. The exact
281 mechanism by which PilZ manipulates PilB AT*Pa*se activity is not yet clear, however the
282 necessity of PilZ binding to PilB for T4P biogenesis has been demonstrated [34] (**Fig. 7**).
283
284 Slightly unexpected is the appearance of a Quorum sensing mutation in the *mvfR* regulator,
285 which is also known as pqsR, a regulator in the Pseudomonas Quinolone Signal (PQS) quorum
286 sensing system. The phage pf, also a T4P binding phage has been shown to generate mutations
287 within the PQS system [35], therefore there is likely some interaction between the PQS system
288 and T4P. Guo et al showed that while adding exogenous PQS did not alter the twitching motility,
289 *pqsR* mutants had attenuated twitching [36]. It is somewhat surprising this mutation was seen
290 in the *SA* positive line. PQS is a pivotal quorum sensing molecule in *PA* that regulates biofilm
291 formation along with a plethora of virulence factors [37]. The role that PQS plays in the killing of
292 *SA* is complex with many PQS regulated factors contributing to *PA*'s competitive advantage. In
293 brief, PQS has antimicrobial properties against *SA*, via the action of 2-heptyl-4-
294 hydroxyquinoline (HHQ) and 2-heptyl-4-hydroxyquinoline N-oxide (HQNO) [38-43]. In PQS
295 mutants (ΔpqsA and ΔpqsH), a reduced ability to kill *SA* has been shown relative to WT *PA*
296 strains [30, 39]. While PQS plays a critical role in *PA*'s ability to kill *SA*, it is part of a complex
297 network of QS molecules and virulence factors influenced by the PQS quorum sensing system.
298 Notably, the antimicrobial activity of PQS and its derivatives is modulated by environmental
299 factors, particularly iron availability [41]. Consequently, competition studies and further
300 investigations using media that more accurately mimic *in vivo* nutrient-limited environments,
301 such as SCFM2, may illuminate potential evolutionary trade-offs or reveal vulnerabilities in
302 Luz19-resistant *PA* harboring *pqsR* mutations.
303
304 These phenotypic and genomic data point us towards the conclusion that Phage Steering was
305 able to work in the presence of *SA* when targeting the T4P. In future work we will expand this to

306 include other bacterial pathogens and commensals, as well as working in media which better
307 mimics infection sites, such as SCFM2. We know that the essential genome of bacteria, as
308 measured by TN-seq, is dependent on environment, both the biotic (inter-species competition)
309 and the abiotic [44]. It is possible that infection environments which include competition from
310 pathogens and commensals, a host immune system, and nutritional limitations might impose to
311 a fitness cost on lost structures which phage can target.
312

313
314 **Figures**

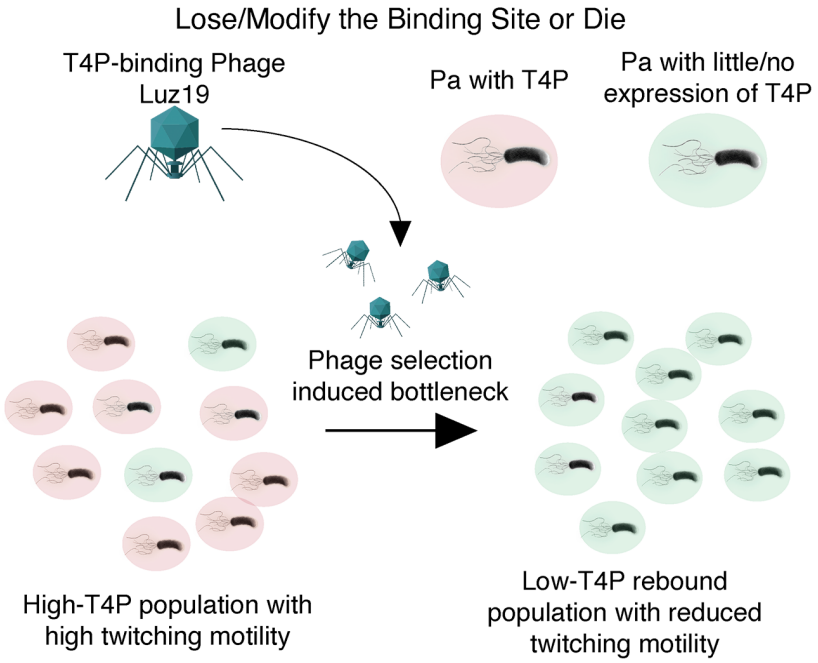

Fig. 1 Phage-steering-mediated selection of Pa populations away from Type IV pilus expression. An initial bacterial population dominated by Pa with Type IV pilus (T4P) expression **(red)** and circulating low T4P-expressing genotypes **(green)**. The T4P-binding bacteriophage, Luz19, acts as a strong selective pressure, selecting for reduced expression of its binding receptor. After phage steering, surviving bacteria are now compromised with reduced expression of the target virulence factor **(green population).**

315
316
317
318
319
320
321
322
323
324
325
326
327
328
329

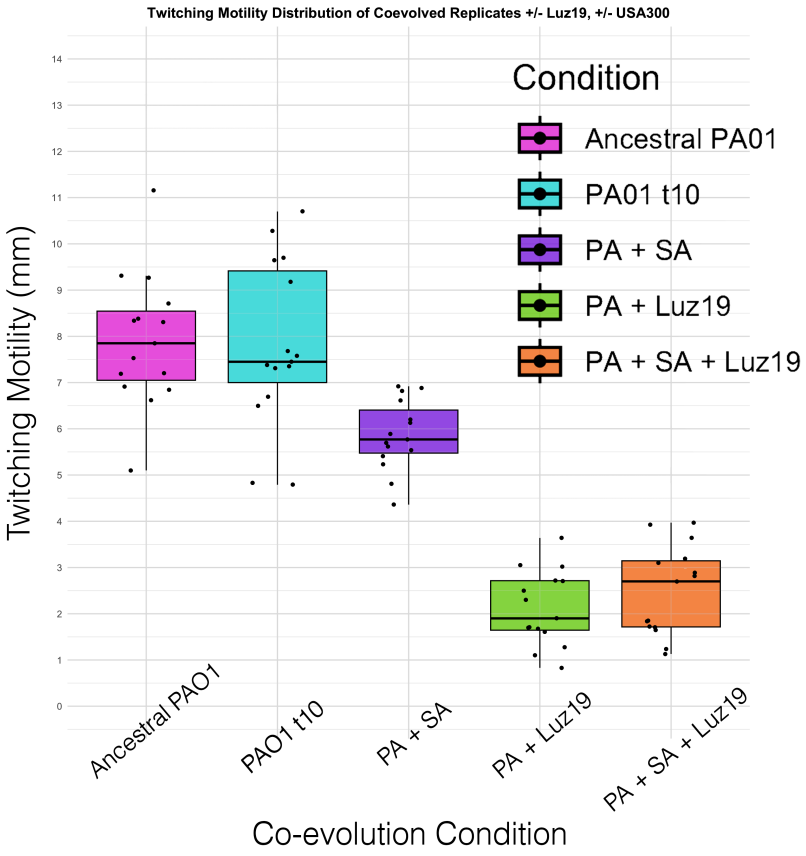

Fig. 2 Twitching motility compared across evolution conditions *PA* twitching motility decreased significantly ($p < 0.05$) in conditions exposed to Luz19 phage relative to the ancestor WT, with no significant difference in twitching motility measured between the positive-phage groups with/without Sa ($p > 0.05$) or between non-phage conditions and the ancestral control $p > 0.05$).

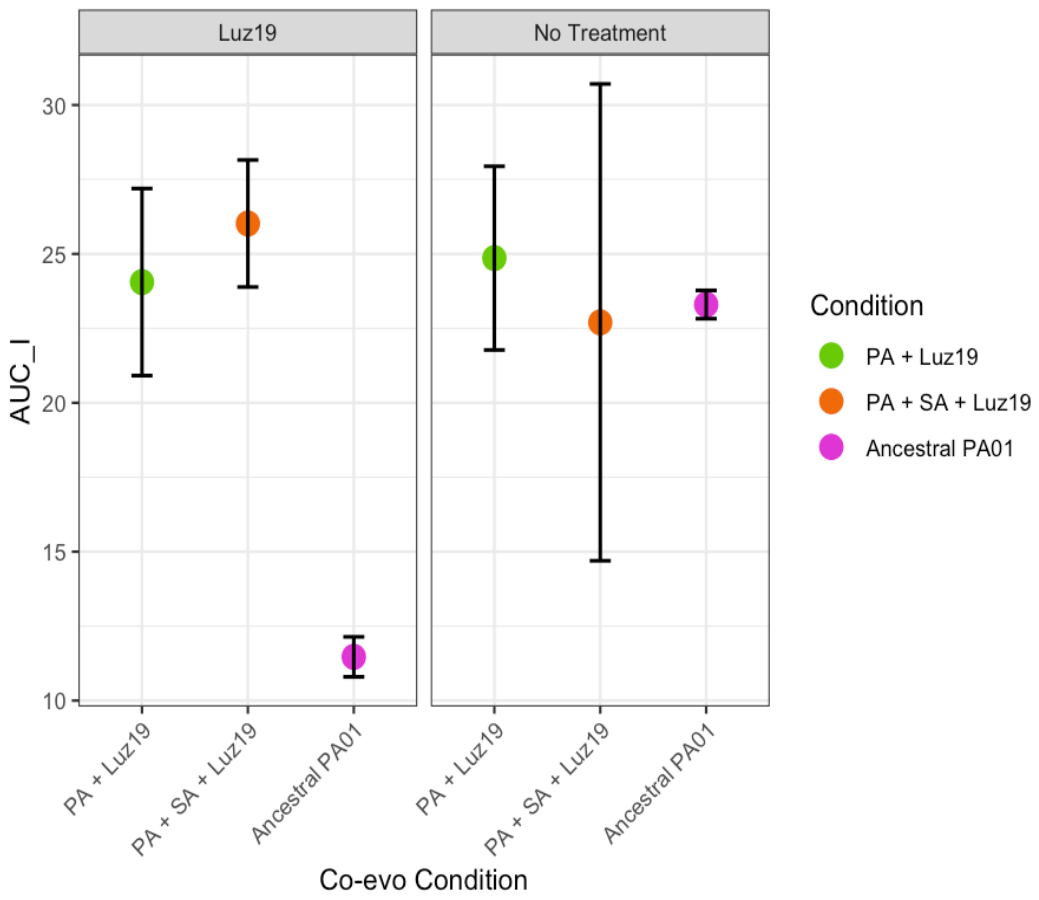

Fig 3. **Growth with and without phage as measured by area under the curve, comparing isolates evolved in the presence of the phage to the ancestor.** Bacteria evolved in the presence of the phage developed resistance to the phage. Area under the curve (AUC_I) was not significantly different with the addition of the ancestor phage when the bacteria had evolved under phage selection.

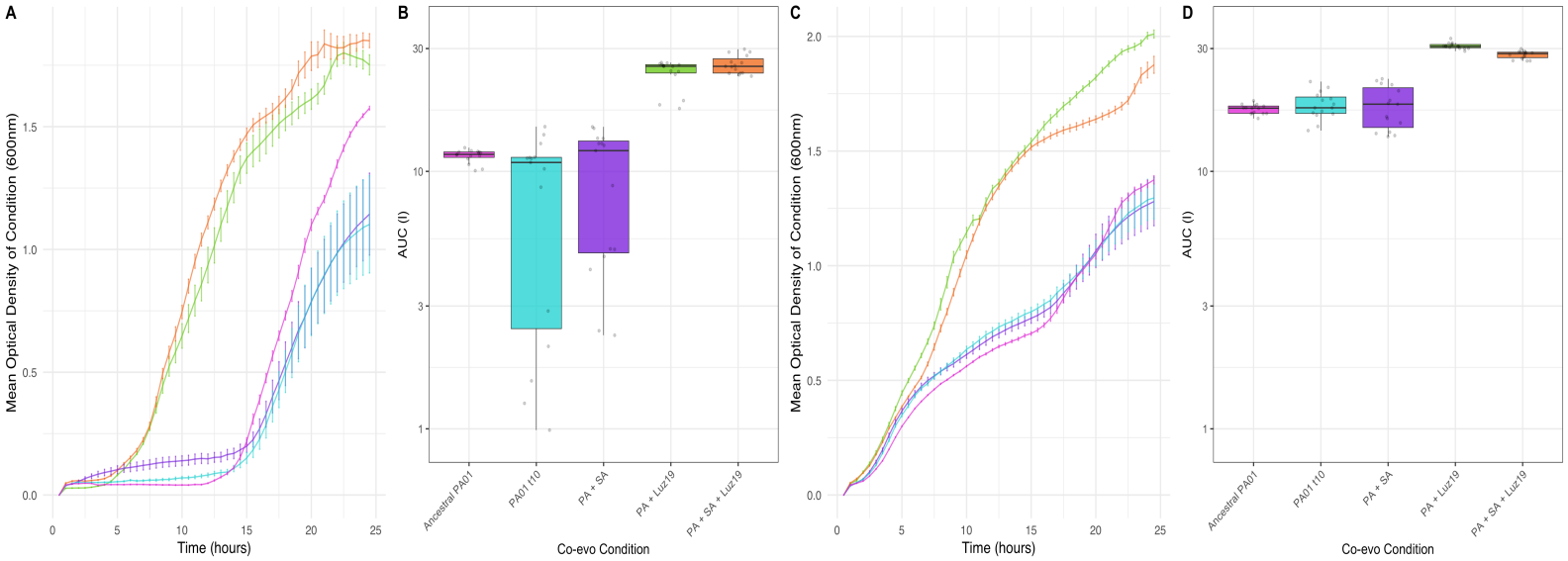

Fig. 4 Growth rate assays and area under the curve (AUC(l)). Growth rate assay mean curves for each co-evolution treatments subject to two different growth rate treatments +Luz19 or +Luz19&*SA*. Area under individual logistic growth curves (AUC(l)), calculated by growthcurver plotted as box plots **A.) Luz19 treatment, growth curve** of the five conditions with Luz19 added to initial inoculation point of cultures at a MOI of 3 (2.67*10^5 PFU). **B.) Luz19 treatment, AUC(l). (Kruskal-Wallis**, χ^2 (4) = **54.54**, p = **4.055***10^-11) **+Luz19** and +SA+Luz19 showed significantly greater AUC(l) in comparison to all other conditions that had not been co-evolved with the phage (**p** < 0.0005**). There was no significant difference between +Luz19 and +Sa+Luz19 (p >** 0.05), **nor between the non-phage-resistant conditions (p** > 0.05) **C.) *S. aureus* & Luz19 treatment, growth curves** of the five conditions with the aforementioned ***PA*:*SA*** ratio and CFUs and Luz19 MOI and PFU. **D) *S. aureus* & Luz19 treatment, AUC(l). (Kruskal-Wallis**, χ^2 (4) = **56.992**, p = **1.242***10^-11) Similarly to the Luz19 treatment (A,**B**), **+Luz19** and +SA+Luz19 showed significantly greater AUC(l) in comparison to all other conditions that had not been co-evolved with the phage (**p** < 0.005**). There was no significant difference between +Luz19 and +Sa+Luz19 (p >** 0.05), **nor between the non-phage-resistant conditions (p** > 0.05).

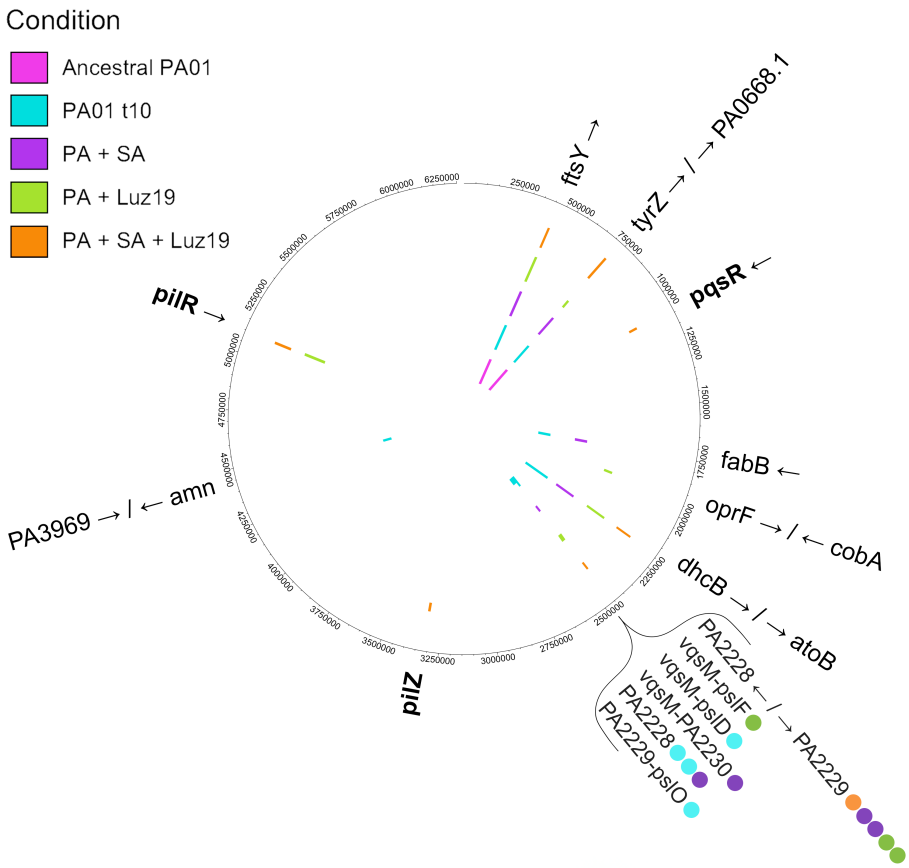

Fig. 5 Chromosomal single nucleotide polymorphisms (SNPs) defined for all coevolution condition replicates and the ancestral wildtype PAO1. SNPs were determined using Breseq. ***pilR***. SNPs of two variations in 5 out of 5 (5/5) *PAO1 + Luz19* co-evo replicates and 3/5 *PAO1 + Sa + Luz19* co-evo replicates. In all but one of these replicate sequences, the SNP in *pilR* is C192Y (TGC→TAC). Replicate b of the +Luz19 condition had a different SNP to *pilR,* P189Q (CCG→CAG). Of the replicates in the two conditions that were subject to co-evolution with Luz19, two lacked a SNP in *pilR,* both in the +Sa+Luz19 condition. Replicate *b* instead had a Δ197 bp deletion in ***pilZ*** . Replicate *a* of +Sa+Luz19 was the only replicate co-evolved alongside Luz19 that sequencing did not reveal a *pil* gene mutation, instead, a PQS system mutation was identified in ***pqsR.***

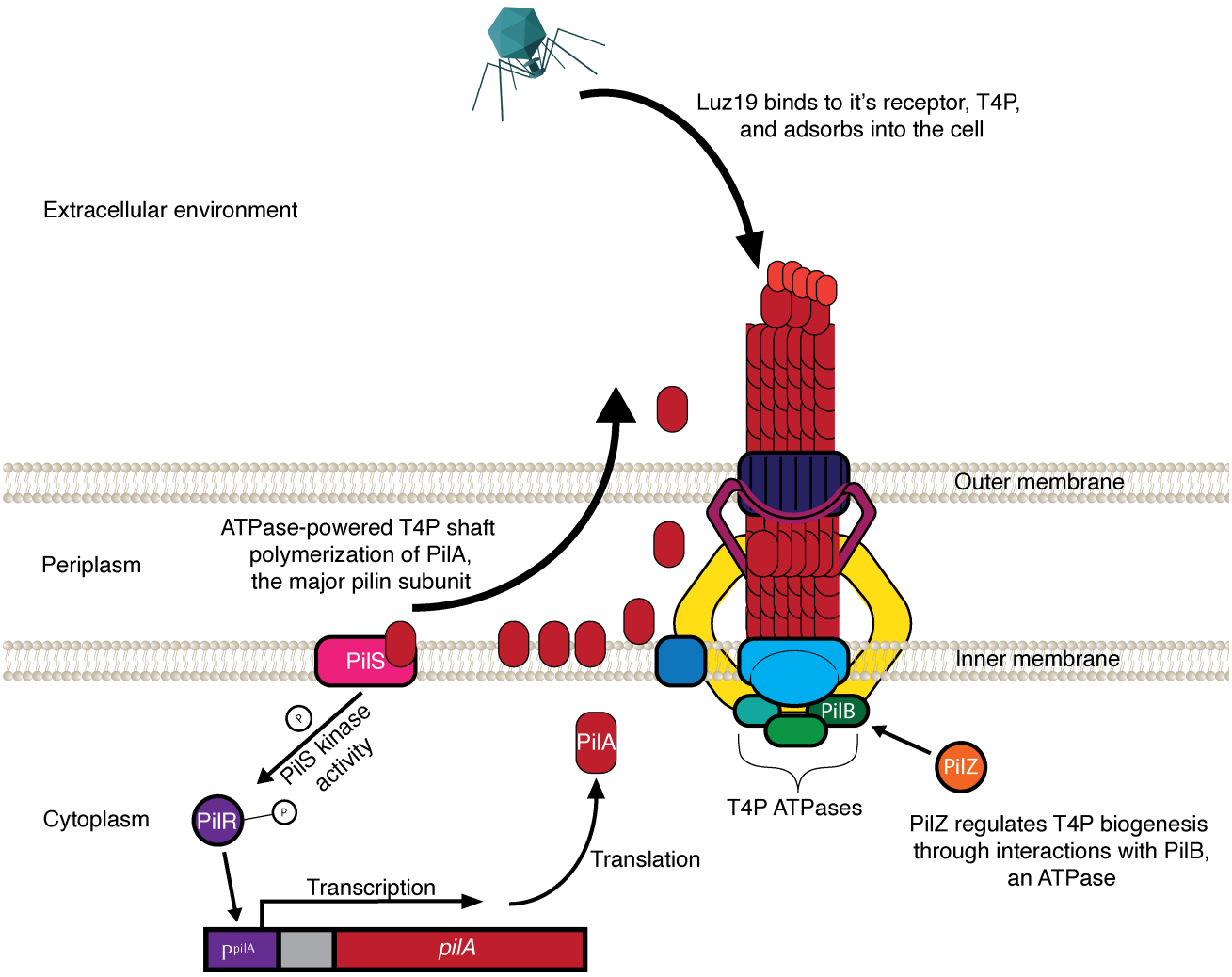

Fig 6. Nominal structure and regulation of the Type IV pilus (T4P) serves as the binding site for Luz19 phage. The assembled T4P shaft is composed of **PilA (red), the major pilin subunit,** and its regulatory mechanisms. The PilSR two-component system controls *pilA* transcription through a phosphorylation signal, with **PilS (pink)** phosphorylating **PilR (purple)** when low PilA concentration localized to the inner-membrane is detected, which then activates *pilA* expression. **PilZ (orange)** is shown interacting with the ATPase, **PilB (green)**, which provides energy for shaft assembly. Luz19 adsorption is dependent of the T4P shaft. This figure represents the wild-type scenario before **mutations that confer** phage resistance.

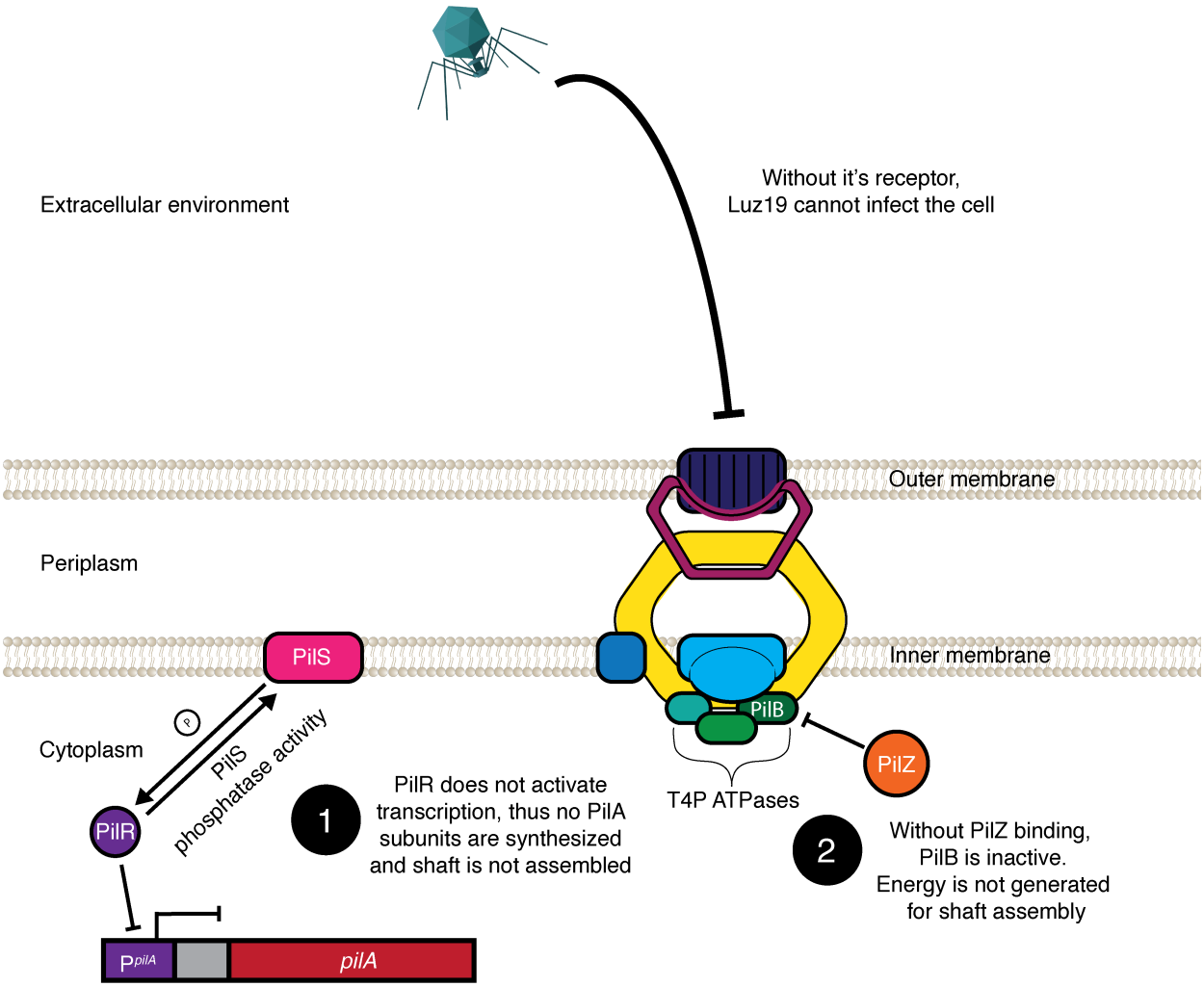

Fig 7. Disrupted Type IV pilus shaft assembly confers phage resistance. This figure demonstrates two key mechanisms preventing pilus formation: **(1)** Inactive **PilR (purple)** fails to activate *pilA* transcription, leading to absence of PilA pilin subunits**. (2**) Failure of **PilZ (orange)** binding renders **PilB (green)** inactive, halting energy production necessary for shaft assembly. The absence of the Type IV pilus shaft is shown, with Luz19 unable to adsorb to the bacterium. Mutations in *pilR* and *pilZ* genes resulted in phage resistance, likely, by preventing pilus formation.

References

1. Betts, A., O. Kaltz, and M.E. Hochberg, *Contrasted coevolutionary dynamics between a bacterial pathogen and its bacteriophages*. Proc Natl Acad Sci U S A, 2014. **111**(30): p. 11109-14.
2. Rohde, C., et al., *Expert Opinion on Three Phage Therapy Related Topics: Bacterial Phage Resistance, Phage Training and Prophages in Bacterial Production Strains*. Viruses, 2018. **10**(4).
3. Medel, R., et al., *Arms Race Coevolution: The Local and Geographical Structure of a Host–Parasite Interaction*. Evolution: Education and Outreach, 2010. **3**(1): p. 26-31.
4. Thompson, J.N., *The geographic mosaic of coevolution*. 2019: University of Chicago Press.
5. Thompson, J.N. and M. Pagel, *Coevolution*. Encyclopedia of Evolution. Oxford University Press, Oxford, 2002.
6. Chao, L., B.R. Levin, and F.M. Stewart, *A Complex Community in a Simple Habitat: An Experimental Study with Bacteria and Phage*. Ecology, 1977. **58**(2): p. 369-378.
7. Horne, M.T., *Coevolution of Escherichia coli and bacteriophages in chemostat culture*. Science, 1970. **168**(3934): p. 992-3.
8. Koskella, B. and M.A. Brockhurst, *Bacteria-phage coevolution as a driver of ecological and evolutionary processes in microbial communities*. FEMS Microbiol Rev, 2014. **38**(5): p. 916-31.
9. Lenski, R.E. and B.R. Levin, *Constraints on the Coevolution of Bacteria and Virulent Phage: A Model, Some Experiments, and Predictions for Natural Communities*. The American Naturalist, 1985. **125**(4): p. 585-602.
10. Schrag, S.J. and J.E. Mittler, *Host-parasite coexistence: the role of spatial refuges in stabilizing bacteria-phage interactions*. The American Naturalist, 1996. **148**(2): p. 348-377.
11. Spanakis, E. and M.T. Horne, *Co-adaptation of Escherichia coli and coliphage lambda vir in continuous culture*. J Gen Microbiol, 1987. **133**(2): p. 353-60.
12. Hall, Alex R., Pauline D. Scanlan, and A. Buckling, *Bacteria-Phage Coevolution and the Emergence of Generalist Pathogens*. The American Naturalist, 2011. **177**(1): p. 44-53.
13. Hall, A.R., et al., *Host-parasite coevolutionary arms races give way to fluctuating selection*. Ecology Letters, 2011. **14**(7): p. 635-642.
14. Gurney, J., et al., *Steering Phages to Combat Bacterial Pathogens*. Trends Microbiol, 2020. **28**(2): p. 85-94.
15. Gurney, J., et al., *Phage steering of antibiotic-resistance evolution in the bacterial pathogen, Pseudomonas aeruginosa*. Evol Med Public Health, 2020. **2020**(1): p. 148-157.
16. DeLeon, S., et al., *Synergistic interactions of Pseudomonas aeruginosa and Staphylococcus aureus in an in vitro wound model*. Infect Immun, 2014. **82**(11): p. 4718-28.

624 17. Hatziagorou, E., et al., *Changing epidemiology of the respiratory bacteriology of*
625 *patients with cystic fibrosis-data from the European cystic fibrosis society patient*
626 *registry.* J Cyst Fibros, 2020. **19**(3): p. 376-383.
627 18. Dalton, T., et al., *An in vivo polymicrobial biofilm wound infection model to study*
628 *interspecies interactions.* PLoS One, 2011. **6**(11): p. e27317.
629 19. Korgaonkar, A., et al., *Community surveillance enhances Pseudomonas aeruginosa*
630 *virulence during polymicrobial infection.* Proc Natl Acad Sci U S A, 2013. **110**(3): p.
631 1059-64.
632 20. Korgaonkar, A.K. and M. Whiteley, *Pseudomonas aeruginosa enhances production*
633 *of an antimicrobial in response to N-acetylglucosamine and peptidoglycan.* J
634 Bacteriol, 2011. **193**(4): p. 909-17.
635 21. Sibley, C.D., et al., *Discerning the complexity of community interactions using a*
636 *Drosophila model of polymicrobial infections.* PLoS Pathog, 2008. **4**(10): p.
637 e1000184.
638 22. Chibeu, A., et al., *The adsorption of Pseudomonas aeruginosa bacteriophage*
639 *phiKMV is dependent on expression regulation of type IV pili genes.* FEMS Microbiol
640 Lett, 2009. **296**(2): p. 210-8.
641 23. Lammens, E., et al., *Representational Difference Analysis (RDA) of bacteriophage*
642 *genomes.* J Microbiol Methods, 2009. **77**(2): p. 207-13.
643 24. Alm, R.A. and J.S. Mattick, *Identification of two genes with prepilin-like leader*
644 *sequences involved in type 4 fimbrial biogenesis in Pseudomonas aeruginosa.* J
645 Bacteriol, 1996. **178**(13): p. 3809-17.
646 25. Weisberg, J.F.a.S., *An {R} Companion to Applied Regression*. Third ed. 2019: Sage.
647 26. Sprouffske, K. and A. Wagner, *Growthcurver: an R package for obtaining*
648 *interpretable metrics from microbial growth curves.* BMC Bioinformatics, 2016. **17**:
649 p. 172.
650 27. Deatherage, D.E. and J.E. Barrick, *Identification of mutations in laboratory-evolved*
651 *microbes from next-generation sequencing data using breseq.* Methods Mol Biol,
652 2014. **1151**: p. 165-88.
653 28. Stover, C.K., et al., *Complete genome sequence of Pseudomonas aeruginosa PAO1,*
654 *an opportunistic pathogen.* Nature, 2000. **406**(6799): p. 959-64.
655 29. Boyd, J.M. and S. Lory, *Dual function of PilS during transcriptional activation of the*
656 *Pseudomonas aeruginosa pilin subunit gene.* J Bacteriol, 1996. **178**(3): p. 831-9.
657 30. Lin, J., et al., *The Pseudomonas Quinolone Signal (PQS): Not Just for Quorum*
658 *Sensing Anymore.* Front Cell Infect Microbiol, 2018. **8**: p. 230.
659 31. Davis, P.B., *Cystic Fibrosis Since 1938.* American Journal of Respiratory and Critical
660 Care Medicine, 2006. **173**(5): p. 475-482.
661 32. Sastry, P.A., et al., *Comparative studies of the amino acid and nucleotide sequences*
662 *of pilin derived from Pseudomonas aeruginosa PAK and PAO.* J Bacteriol, 1985.
663 **164**(2): p. 571-7.
664 33. Strom, M.S. and S. Lory, *Mapping of export signals of Pseudomonas aeruginosa pilin*
665 *with alkaline phosphatase fusions.* J Bacteriol, 1987. **169**(7): p. 3181-8.

34. Guzzo, C.R., et al., *PILZ Protein Structure and Interactions with PILB and the FIMX EAL Domain: Implications for Control of Type IV Pilus Biogenesis*. Journal of Molecular Biology, 2009. **393**(4): p. 848-866.
35. Schwartzkopf, C.M., et al., *Inhibition of PQS signaling by the Pf bacteriophage protein PfsE enhances viral replication in Pseudomonas aeruginosa*. Mol Microbiol, 2024. **121**(1): p. 116-128.
36. Guo, Q., et al., *PqsR-dependent and PqsR-independent regulation of motility and biofilm formation by PQS in Pseudomonas aeruginosa PAO1*. Journal of Basic Microbiology, 2014. **54**(7): p. 633-643.
37. Pesci, E.C., et al., *Quinolone signaling in the cell-to-cell communication system of Pseudomonas aeruginosa*. Proc Natl Acad Sci U S A, 1999. **96**(20): p. 11229-34.
38. Filkins, L.M., et al., *Coculture of Staphylococcus aureus with Pseudomonas aeruginosa Drives S. aureus towards Fermentative Metabolism and Reduced Viability in a Cystic Fibrosis Model*. J Bacteriol, 2015. **197**(14): p. 2252-64.
39. Haussler, S. and T. Becker, *The pseudomonas quinolone signal (PQS) balances life and death in Pseudomonas aeruginosa populations*. PLoS Pathog, 2008. **4**(9): p. e1000166.
40. Nairz, M., et al., *The struggle for iron - a metal at the host-pathogen interface*. Cell Microbiol, 2010. **12**(12): p. 1691-702.
41. Nguyen, A.T., et al., *Cystic Fibrosis Isolates of Pseudomonas aeruginosa Retain Iron-Regulated Antimicrobial Activity against Staphylococcus aureus through the Action of Multiple Alkylquinolones*. Front Microbiol, 2016. **7**: p. 1171.
42. Nguyen, A.T. and A.G. Oglesby-Sherrouse, *Interactions between Pseudomonas aeruginosa and Staphylococcus aureus during co-cultivations and polymicrobial infections*. Appl Microbiol Biotechnol, 2016. **100**(14): p. 6141-6148.
43. Otto, B.R., A.M. Verweij-van Vught, and D.M. MacLaren, *Transferrins and heme-compounds as iron sources for pathogenic bacteria*. Crit Rev Microbiol, 1992. **18**(3): p. 217-33.
44. Ibberson, C.B., et al., *Co-infecting microorganisms dramatically alter pathogen gene essentiality during polymicrobial infection*. Nat Microbiol, 2017. **2**: p. 17079.